Available online at www.sciencedirect.com
ScienceDirect
Virology 371 (2008) 362–373
VIROLOGY
www.elsevier.com/locate/yviro

Circularization of an RNA template via long-range base pairing is critical for hepadnaviral reverse transcription

Myeong-Kyun Shin [1], Jong-Hoon Kim [1], Dong-Kyun Ryu, Wang-Shick Ryu *

Department of Biochemistry, Yonsei University, 134 Shinchondong, Seodaemungu, Seoul, 120-749, South Korea

Received 25 July 2007; returned to author for revision 15 September 2007; accepted 27 September 2007
Available online 7 November 2007

Abstract

Although an overall genetic strategy for hepadnaviral reverse transcription has been established, the mechanism that underlies the minus-strand transfer is still poorly defined. We and others independently identified a novel *cis*-acting element, termed β or ϕ, respectively, that is critical for the minus-strand DNA synthesis of hepatitis B virus. A 5′–3′, long-range interaction of the RNA template was proposed that involves the 5′ ε sequence (encapsidation signal) and the 3′ β/ϕ sequence. We subjected the hypothesized base pairing to genetic analysis. The data indicated that mutations abrogating the hypothesized base pairing markedly impaired minus-strand DNA synthesis, while compensatory mutations that restored the base pairing rescued the minus-strand DNA synthesis. These results demonstrated the critical role of the 5′–3′, long-range interaction in minus-strand DNA synthesis. We speculate that such a long-range interaction may precisely juxtapose a donor to an acceptor during minus-strand transfer.

Keywords: Hepatitis B virus; Reverse transcription; Minus-strand DNA synthesis

Introduction

Human hepatitis B virus (HBV) is a member of the hapadnavirus family of small, enveloped, animal DNA viruses (Ganem and Schneider, 2001). Other members of the family include the duck hepatitis B virus (DHBV) and the woodchuck hepatitis virus (WHV). HBV is a major cause of liver disease worldwide, ranging from acute and chronic hepatitis to liver cirrhosis and hepatocellular carcinoma.

The hepadnaviruses are unique among the animal DNA viruses in that they replicate through reverse transcription of an RNA intermediate. The strategy of hepadnaviral reverse transcription parallels that of retroviruses to some degree. For instance, both reverse transcription reactions require multiple template switching events for the completion of viral genome replication. In addition, these template switching events are mediated primarily through complementary sequences in the terminal redundancy regions of their RNA genomes (Dang and Hu, 2001; Nassal and Rieger, 1996; Tavis et al., 1994).

Hepadnaviral reverse transcription occurs inside nucleocapsids that follow selective encapsidation of the pregenomic RNA (pgRNA). Encapsidation proceeds by recognition of a stem-loop structure (encapsidation signal or ε) near the 5′ end of the pgRNA by the viral polymerase (P) (Hirsch et al., 1991; Junker-Niepmann et al., 1990). Initiation of minus-strand DNA synthesis occurs through a novel mechanism during which P itself acts as a primer by forming a covalent linkage with the first nucleotide of the DNA (Wang and Seeger, 1992); the template for this priming reaction is a bulge of 5′ ε (Fig. 1) (Nassal and Rieger, 1996; Tavis et al., 1994; Wang and Seeger, 1993). In other words, the P protein directs the packaging of the pgRNA as well as the priming, and 5′ ε serves not only as an encapsidation signal but also as the initiation site for minus-strand DNA synthesis. The fact that both P and 5′ ε play pivotal roles in the priming reaction as well as in encapsidation suggests that the initiation of minus-strand DNA synthesis is mechanistically coupled to pgRNA encapsidation.

Our current understanding of hepadnaviral minus-strand transfer is far from complete. Minus-strand DNA synthesis, the first step of hepadnaviruses reverse transcription, features two characteristic processes—protein priming and minus-strand transfer. Following synthesis of the first 3 or 4 nucleotides via protein priming, the P-linked oligonucleotide translocates from

* Corresponding author. Fax: +82 2 362 9897.
E-mail address: wsryu@yonsei.ac.kr (W.-S. Ryu).
[1] These authors contributes equally to this work.

0042-6822/$ - see front matter © 2007 Elsevier Inc. All rights reserved.
doi:10.1016/j.virol.2007.09.042

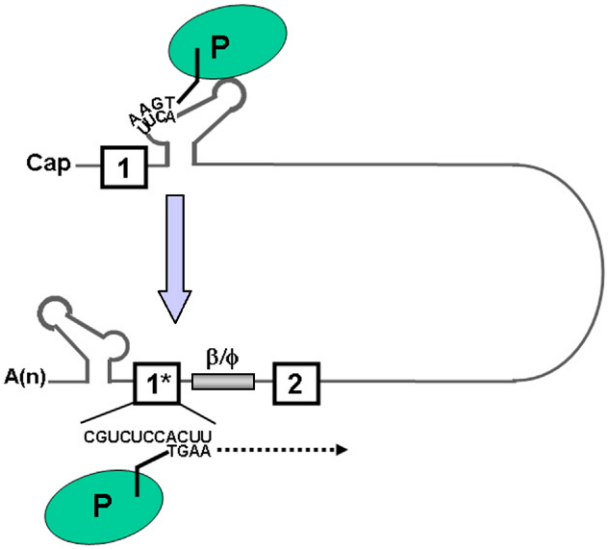

Fig. 1. Schematic diagram depicting minus-strand transfer during hepadnaviral reverse transcription. The pgRNA with *cis*-acting elements relevant to minus-strand transfer is shown. The open boxes represent direct repeat sequences of 11 nucleotides, designated 1 and 2 (i.e., DR1 and DR2); DR1 is present twice due to terminal redundancy and the DR nearest the 3′ end is designated DR1*. The encapsidation signal (ε) near the 5′ terminus, which folds into a stem-loop structure, is shown. The viral P protein (shaded oval) synthesizes the first 3 or 4 nucleotides of minus-strand DNA by using the UUCA sequence within the bulge of the stem-loop structure as a template. The P protein, covalently linked to the oligonucleotide, is transferred to the UUCA at DR1*, which is referred to as an acceptor, and then resumes minus-strand DNA synthesis. A gray box denotes a *cis*-acting element, referred to as the β/ϕ sequence. Figure is not drawn to scale.

the donor (i.e., bulge of 5′ ε, a stem-loop structure) to the acceptor site [i.e., the UUC motif of the 3′ DR1 (direct repeat) or DR1*] at the opposite end, where minus-strand DNA synthesis resumes (Fig. 1). This process is termed minus-strand transfer or template switching (Pollack and Ganem, 1994; Tavis et al., 1994; Wang and Seeger, 1993). An immediate question arises of how accurate transfer to the UUC motif of DR1* can be ensured. Intriguingly, in DHBV, a juxtaposition of the donor and acceptor sites during minus-strand transfer has been implicated by observation of a marked preference for the wild-type acceptor site over other nearby UUC motifs (Loeb and Tian, 1995). Subsequently, such juxtapositions that could occur via circularization of the pre-genome were suggested to explain how strand transfer occurs (Rieger and Nassal, 1996). Circularization can be achieved either by 5′–3′, long-range RNA-RNA interactions or by RNA-protein interactions.

Recently, we and others independently identified a novel *cis*-acting sequence – a 28-nucleotide sequence located upstream of DR1* – that is required for minus-strand DNA synthesis (Shin et al., 2004; Tang and McLachlan, 2002), and termed β or ϕ, respectively (Fig. 1). The two reported sequences most likely represent an identical *cis*-acting element (here referred to as β/ϕ), since mutants with alterations in these sequences manifested an indistinguishable phenotype (Shin et al., 2004; Tang and McLachlan, 2002), and these two *cis*-acting elements essentially overlap. To account for the role of the β/ϕ element, we previously hypothesized that the β element contributes to the accurate and efficient minus-strand transfer (Shin et al., 2004). Intriguingly, Tang and McLachlan (2002) hypothesized a novel circular structure of the pgRNA formed via significant base pairing between the 5′ ε and the β/ϕ sequences. In support of the latter hypothesis, we now present evidence for the 5′–3′, long-range interaction that could occur during minus-strand DNA synthesis. Similar conclusions have recently been reported by others (Abraham and Loeb, 2006; Oropeza and McLachlan, 2007). Additional deletion analysis defined a short, 7-nucleotide RNA sequence, immediately adjacent to UUCA at DR1*, which is an important determinant in selecting the wild-type acceptor site of DR1* during minus-strand transfer.

Results

Experimental strategy

As stated above, a novel *cis*-acting sequence, adjacent to the acceptor site and independently termed the ϕ or β sequence, was identified (Shin et al., 2004; Tang and McLachlan, 2002). However, it remains to be established how the β/ϕ sequence contributes to minus-strand DNA synthesis. Tang and McLachlan (2002) proposed a novel circular structure of the pgRNA that was mediated by significant base pairing between the 5′ ε and ϕ sequences (Fig. 2B). Importantly, the proposed structure that brings the donor and acceptor into proximity appeared to be conserved among hepadnaviruses (Tang and McLachlan, 2002). To evaluate this model, we subjected the hypothesized base pairing to stringent genetic analysis. Briefly, the first step was to identify multiple substitution mutants in the 5′ ε stem-loop structure that are competent for encapsidation but fail to yield viral DNA. The next step was to determine whether a compensatory mutation that recovers the base pairing could restore DNA synthesis. In fact, the process of pgRNA encapsidation was shown to be extremely sensitive to alterations in the secondary structure as well as primary sequence of 5′ ε (Fallows and Goff, 1995; Pollack and Ganem, 1993). It was noted, however, that a region on the left side of the upper stem was found to be tolerant of substitution (Fallows and Goff, 1995; Pollack and Ganem, 1993) (Fig. 2A). Therefore, this region was subjected to genetic analysis. We reasoned that ablation of 3 out of 9 base pairs would be sufficient to destabilize the upper portion of the hypothesized structure (Fig. 2A) since a similar extent of substitution was sufficient to impair the encapsidation function of DHBV ε (Pollack and Ganem, 1993). We generated three 3-nucleotide substitutions and one 4-nucleotide substitution on the left side of the upper stem (Fig. 3A).

The mutations at 5′ ε are impaired in the minus-strand DNA synthesis

We first confirmed normal encapsidation of the four mutants. HBV DNA replicons of each mutant were transfected into Huh7 cells along with a helper plasmid, R063. The helper plasmids were cotransfected to provide C (core), P (polymerase) in *trans* to ensure that their amounts were not limiting (Shin et al., 2004). To prevent the degradation of the pgRNA by the RNase H activity associated with the P protein, cells were treated with lamivudine for 2 days, an established inhibitor of the viral reverse transcriptase (Ono

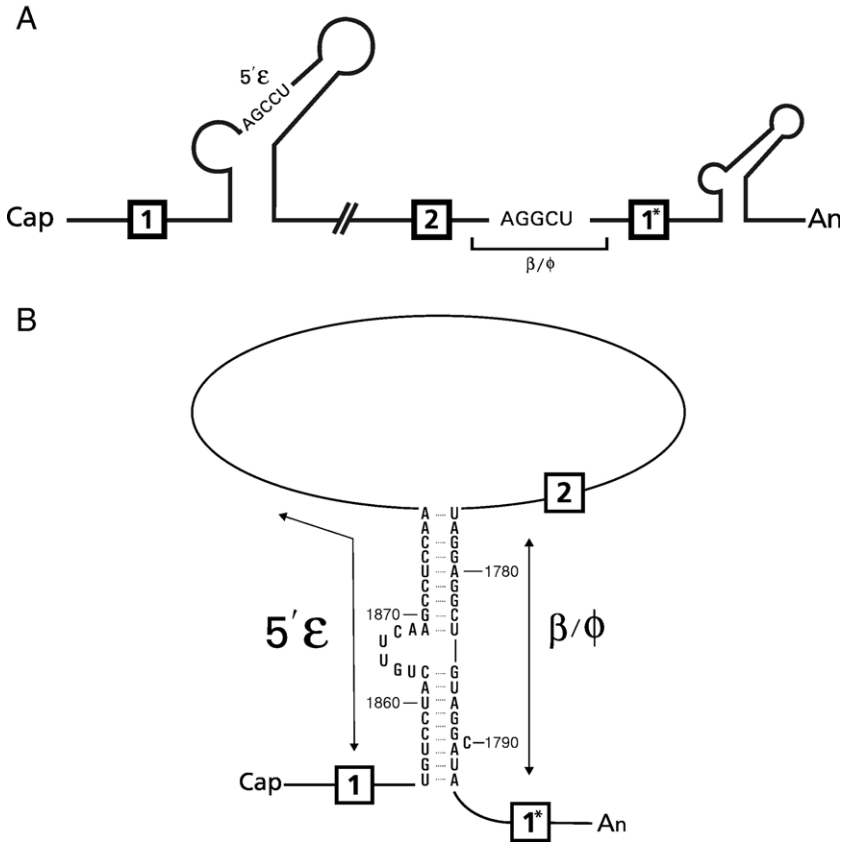

Fig. 2. Schematic diagram depicting the hypothesized base pairing between the 5′ ε and β/ϕ sequences. (A) The pregenomic RNA is illustrated schematically with only relevant nucleotide sequence in 5′ ε and β/ϕ region. (B) The pregenomic RNA is depicted with emphasis on the hypothesized base pairing. Double-arrowed lines denote the region spanning the 5′ ε and β/ϕ sequences, respectively. Notably, the 5′ ε bulge on the left side of the base pairing structure remains unpaired. Although the size (6 nt) of the bulge region remains unchanged, it is noted that the bulge region shifted one nucleotide toward the 3′ end, relative to the stem-loop structure (see Fig. 1). Symbols are as in Fig. 1.

et al., 2001). Three days post-transfection, RNA was extracted from capsid and cytoplasm, respectively. The pgRNA was analyzed by RNase protection analysis (RPA), as described previously (Shin et al., 2004). RPA data, shown in Fig. 3B, indicated that pgRNAs derived from all mutants were normally encapsidated, as anticipated from previous result (Fallows and Goff, 1995). Next, we examined whether these mutants supported the viral genome replication.

Nucleocapsids that contained the viral replication intermediates were isolated from cells transfected with each mutant DNA and the capsid-associated DNAs were then analyzed by Southern blot analysis (Fig. 3C). As anticipated, transfection of the wild-type HBV construct yielded three major replication intermediates: relaxed circular DNA (RC), duplex linear DNA (DL) and single-stranded DNA (SS) (Fig. 3C, lane 1). By contrast, the amounts of the viral DNAs produced by all mutants were markedly diminished (Fig. 3C, lane 1 versus lanes 2 to 5). To obtain a more quantitative estimation, we carried out primer extension analysis to measure the minus-strand DNA that was initiated at DR1*, as previously described (Shin et al., 2004). The data shown in Fig. 3, panels D and E, indicated that minus-strand DNA synthesis was substantially reduced in all mutants compared to the wild type. Transfection into a different hepatoma cell line, HepG2, yielded essentially identical results (data not shown). Further, the results were in accordance with those of the Southern blot analysis shown above. Therefore, we concluded that all four mutants, bearing substitutions on the left side of the upper stem, were unimpaired in encapsidation but severely impaired in minus-strand DNA synthesis.

Compensatory mutations rescue the viral DNA synthesis

Nonetheless, we did not know whether the mutants were defective in protein priming or in subsequent minus-strand transfer. We considered two possibilities to which the substituted region could contribute. First, the substituted region constituted a core element that was recognized by the P protein, which is critical for the priming reaction (Schaaf et al., 1999). Second, the substituted region possessed a novel function that is critical for minus-strand transfer. We decided to examine the latter possibility by evaluation of the hypothesized base pairing shown in Fig. 2B. We generated a set of compensatory substitutions (double-site mutations) that restored the base pairing that had been ablated by the initial substitutions (single-site mutations) (Fig. 4A). It was expected that the double-site mutations could rescue viral DNA synthesis if only the hypothesized base pairing contributed to minus-strand DNA synthesis.

Four double-site mutant DNAs were transfected and analyzed similarly as described above. First, RPA was carried out as shown in Fig. 3B. RPA data confirmed that encapsidation proceeded

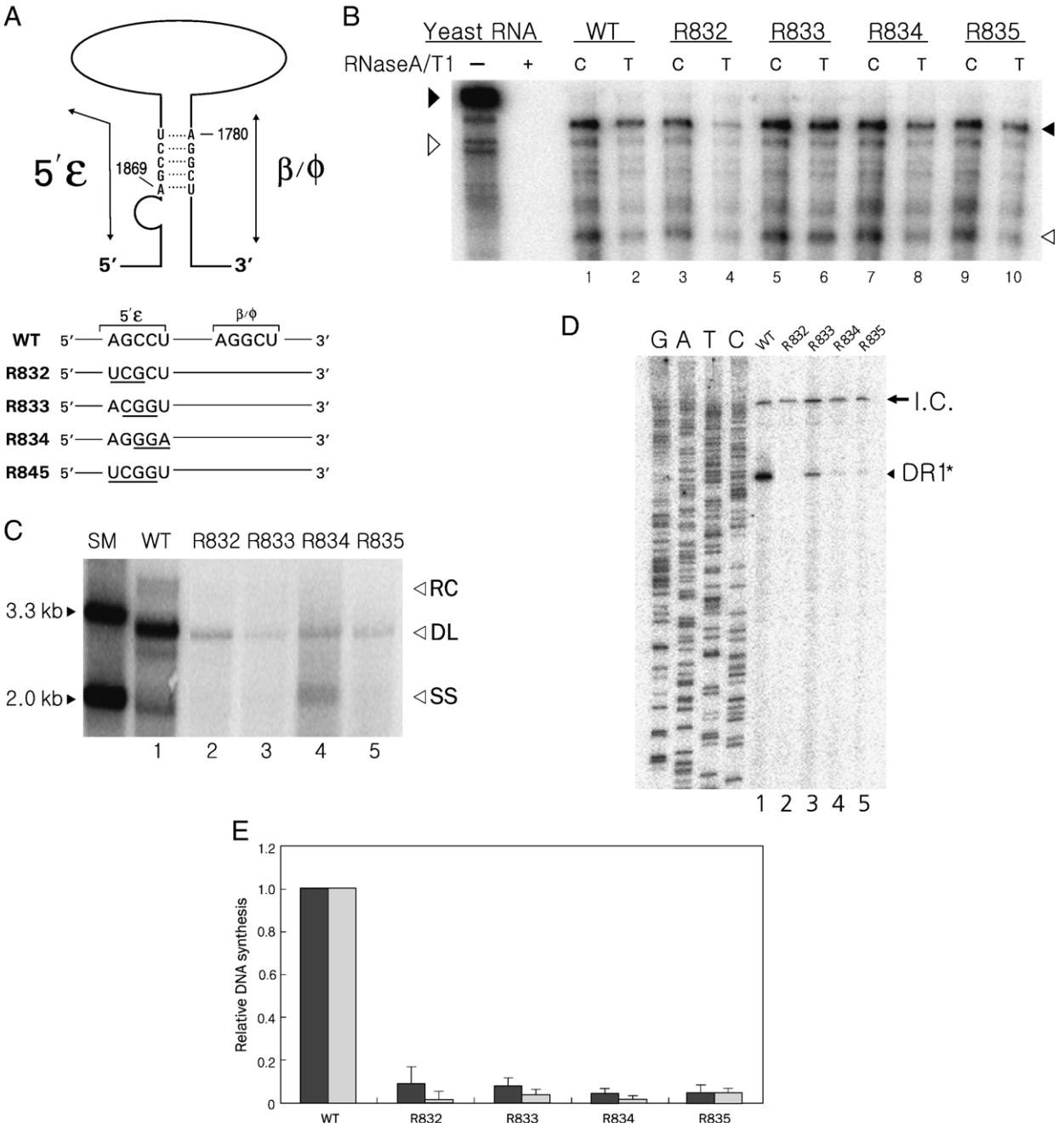

Fig. 3. Mutants with substitutions on the left side of the upper-stem of the hypothesized structure were competent for encapsidation but failed to yield minus-strand DNA. (A) Schematic diagram showing the hypothesized base pairing between the 5′ ε and β/ϕ sequences along with nucleotide sequences substituted in the mutants. Nucleotide sequences of four mutants are presented below, with altered bases underlined. (B) RNase protection analysis was carried out to examine the encapsidation efficiency. Cells were cotransfected with each substitution mutant or wild type, as indicated above each lane, along with a helper plasmid, R063, as detailed in Materials and methods. On next day, transfected cells were treated with lamivudine (20 μM, LG Life Science Inc., Korea). pLZ-ε-30 plasmid that transcribes a LacZ transcript capable of being encapsidated was cotransfected as an internal control, as described (Shin et al., 2004). The protected RNA fragments, derived from HBV RNA and the *lacZ* transcript, are indicated by closed and open, left-facing arrowheads, respectively. The probes used for the analysis of HBV RNA and the *lacZ* RNA are indicated by closed and open, right-facing arrowheads, respectively. Yeast RNA shown in two leftmost lanes was used as a nonspecific RNA control. One fifth of the RNAs extracted from total cells (T) were loaded relative to those of capsids (C). Representative results of at least three experiments are shown. (C) Southern blot analysis of the replication-intermediate DNAs extracted from cytoplasmic core particles. Cells were transfected with each substitution mutant or wild type (WT), along with the helper plasmid, R063. The positions of RC, DL and SS DNA are indicated by open arrowheads. Two restriction fragments of 3.3 and 2.0 kb serve as size markers (SM). For a comparison, only one tenth of the extracted DNA from the wild type was loaded relative to those of the mutants. Representative results of at least five experiments are shown. (D) Primer extension analysis. Primer extension analysis was performed to measure the amount of minus-strand DNA initiated at DR1*, as described in Materials and methods. The position of the extended products derived from the DNA initiated at DR1* is denoted by a closed arrowhead. I.C.: internal control. Representative results of at least three experiments are shown. (E) Quantitative analysis. Relative DNA synthesis by each mutant was estimated by normalizing the amounts of viral DNAs, as determined by Southern blot analysis (dark) or primer extension analysis (gray), to the amount of the encapsidated RNA detected in the capsid that has been normalized to the encapsidated LacZ transcript, as performed previously (Shin et al., 2004). Error bars represent standard deviations from five independent transfections.

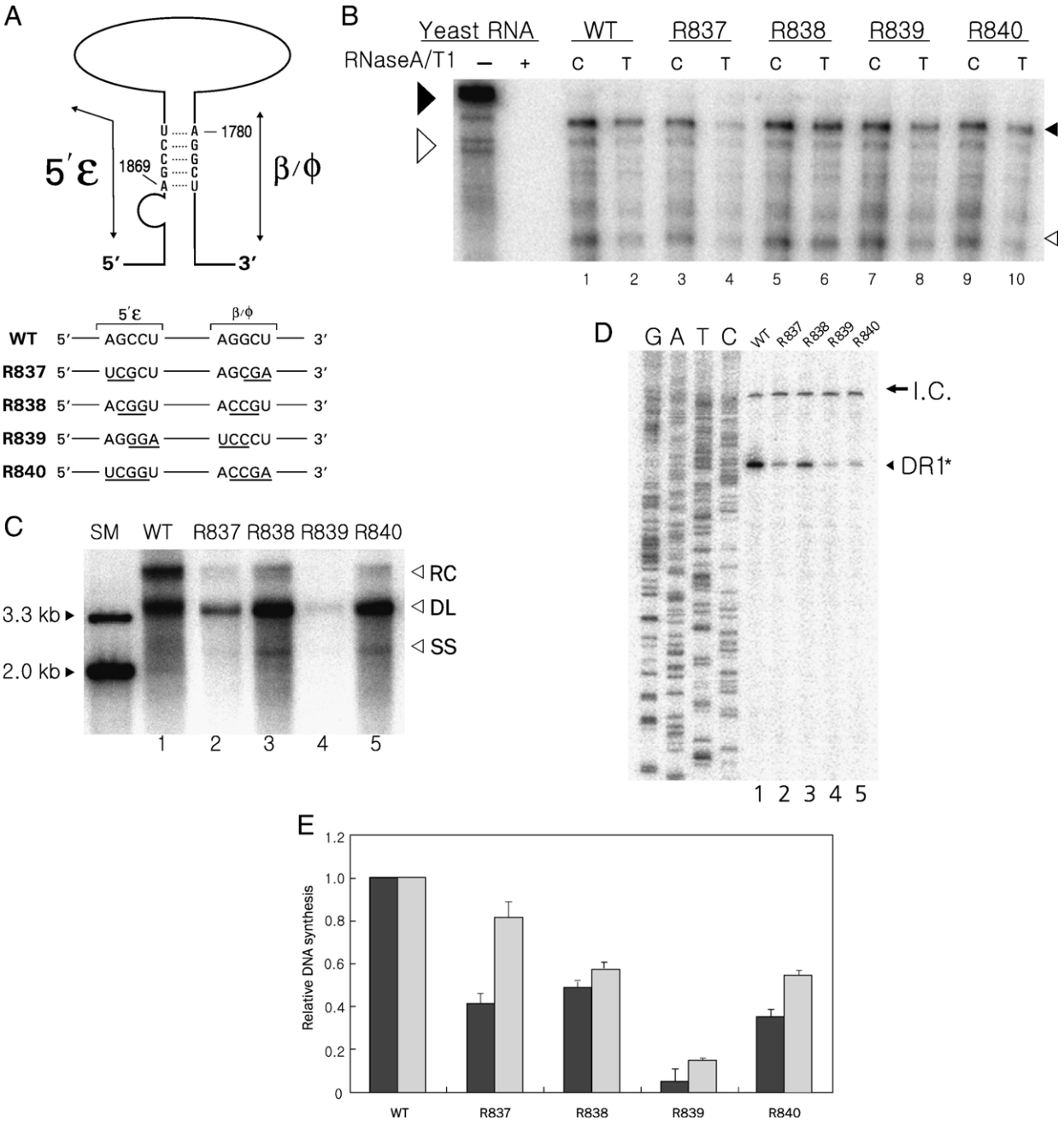

Fig. 4. Compensatory substitutions rescued minus-strand DNA synthesis. (A) Schematic diagram showing the hypothesized base pairing between the 5′ ε and β/ϕ sequences along with a strategy for compensatory substitution mutagenesis. Nucleotide sequences of four mutants with a compensatory substitution mutation are presented below with only altered bases underlined. Symbols are as in Fig. 3A. (B) RPA analysis was performed as described in the legend for Fig. 3B. (C) Southern blot analysis was performed as described in the legend for Fig. 3C, except that all samples were equally loaded. (D) Primer extension analysis was performed as shown in Fig. 3D. (E) Quantitative analysis. Quantitation was carried out as detailed in Fig. 3E. Error bars represent standard deviations from four or more independent transfections.

normally in all mutants having the double-site mutation (Fig. 4B). Remarkably, Southern blot analysis indicated that a set of mutants that had compensatory substitutions, with the possible exception of mutant R839, markedly rescued the viral DNA synthesis (Fig. 4C versus Fig. 3C). Primer extension analysis indicated that the minus-strand DNA synthesis initiated at DR1* in all mutants was substantially restored (Fig. 4D), in accordance with that of Southern blot analysis. Overall, quantitative estimation that followed normalization of encapsidated RNA supported the notion that the base pairing between the 5′ ε and β/ϕ sequences is critical for the synthesis of minus-strand DNA (Fig. 4E).

On the other hand, quantitative estimation revealed that in the case of R839, minus-strand DNA synthesis was not substantially recovered, unlike to those of the other three mutants (Fig. 4E). It is possible that the priming reaction could be affected by a residue that is altered only in mutant R839 (i.e., nt 1873 U), but not in other mutants (Fig. 3A). Unlike its DHBV counterpart (Schaaf et al., 1999), the inability to recapitulate the protein priming reaction *in*

vitro by using HBV polymerase did not allow us to address this question further.

The mutations at 3′ β/ϕ region are impaired in the minus-strand DNA synthesis

To substantiate the above finding, it is crucial to demonstrate that a single site mutation in 3′ β/ϕ region is defective as well for the minus-strand DNA synthesis. To this end, we generated a series of corresponding single site mutation in 3′ β/ϕ region and measured the extent to which these mutants are impaired in the minus-strand DNA synthesis (Fig. 5A). First, we sought to confirm that encapsidation proceeds normally in these mutants. RPA was carried out as shown in Fig. 3B. As anticipated, RPA indicated that encapsidation proceeds normally in these 3′ β/ϕ region mutants (Fig. 5B). Nonetheless, Southern blot analysis

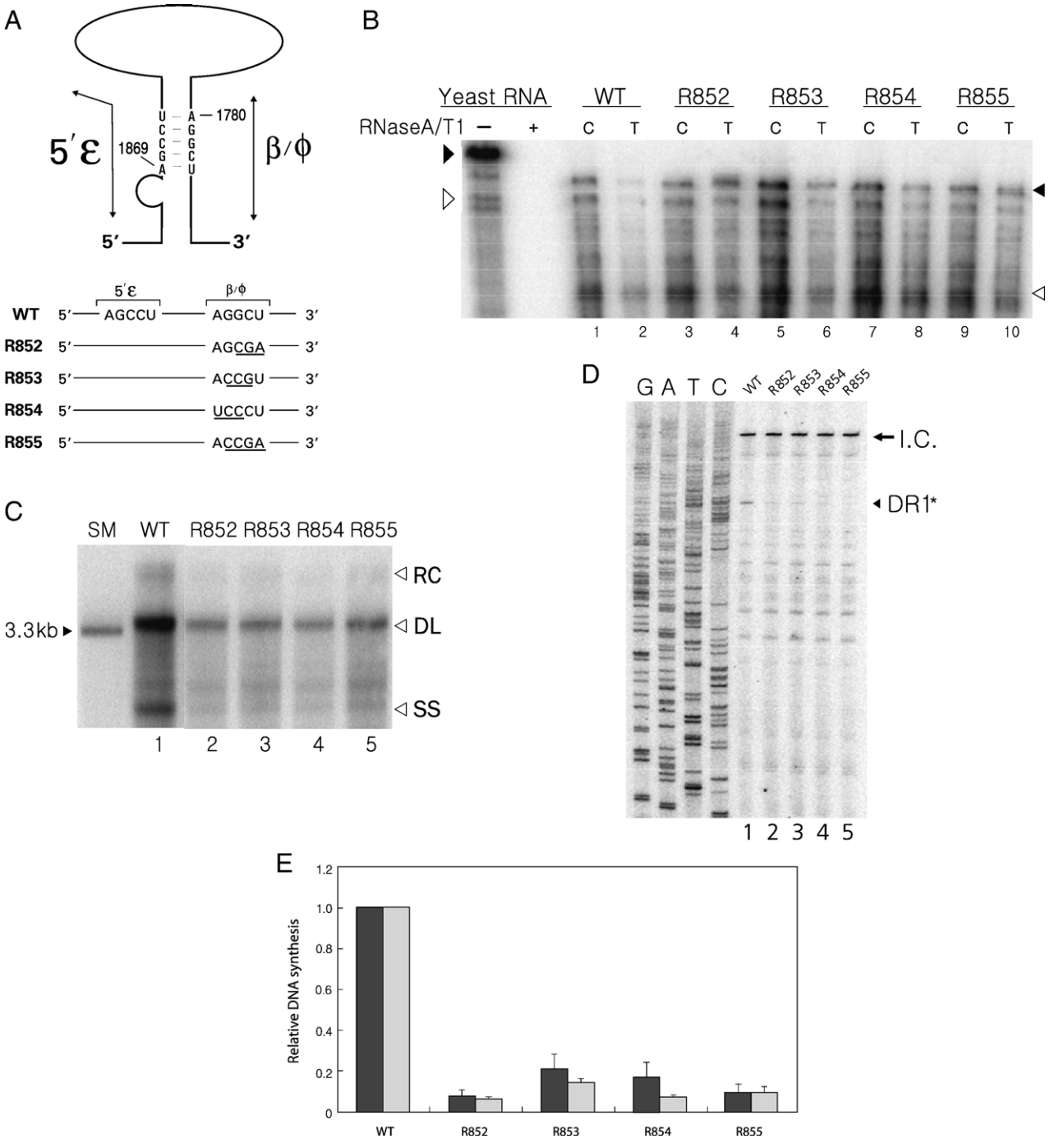

Fig. 5. Mutants in the β/ϕ sequences are defective for the minus-strand DNA synthesis. (A) Schematic diagram showing a single site mutation in the β/ϕ sequences. Symbols are as in Fig. 3A. (B) RPA analysis was performed as described in the legend for Fig. 3B. Only one fifth of the RNAs extracted from total cells (T) were loaded relative to those of capsids (C). (C) Southern blot analysis was performed as described in the legend for Fig. 4C. (D) Primer extension analysis was performed as shown in Fig. 3D. (E) Quantitative analysis as shown in Fig. 3E. Error bars represent standard deviations from three independent transfections.

demonstrated that the DNA synthesis appeared to be significantly reduced in all four mutants (Fig. 5C). Likewise, primer extension analysis showed that the minus-strand DNA synthesis was significantly reduced in these mutants (Fig. 5D). Normalization to the level of the encapsidated RNA revealed that four single site mutants in 3′ β/ϕ region are severely defective in the minus-strand DNA synthesis (Fig. 5E), although the extent of the defect of the 3′ β/ϕ region mutants was lesser than those of the 5′ ε region mutants (Fig. 3E versus Fig. 5E). It appeared that the single site mutations in the 5′ ε sequence were more

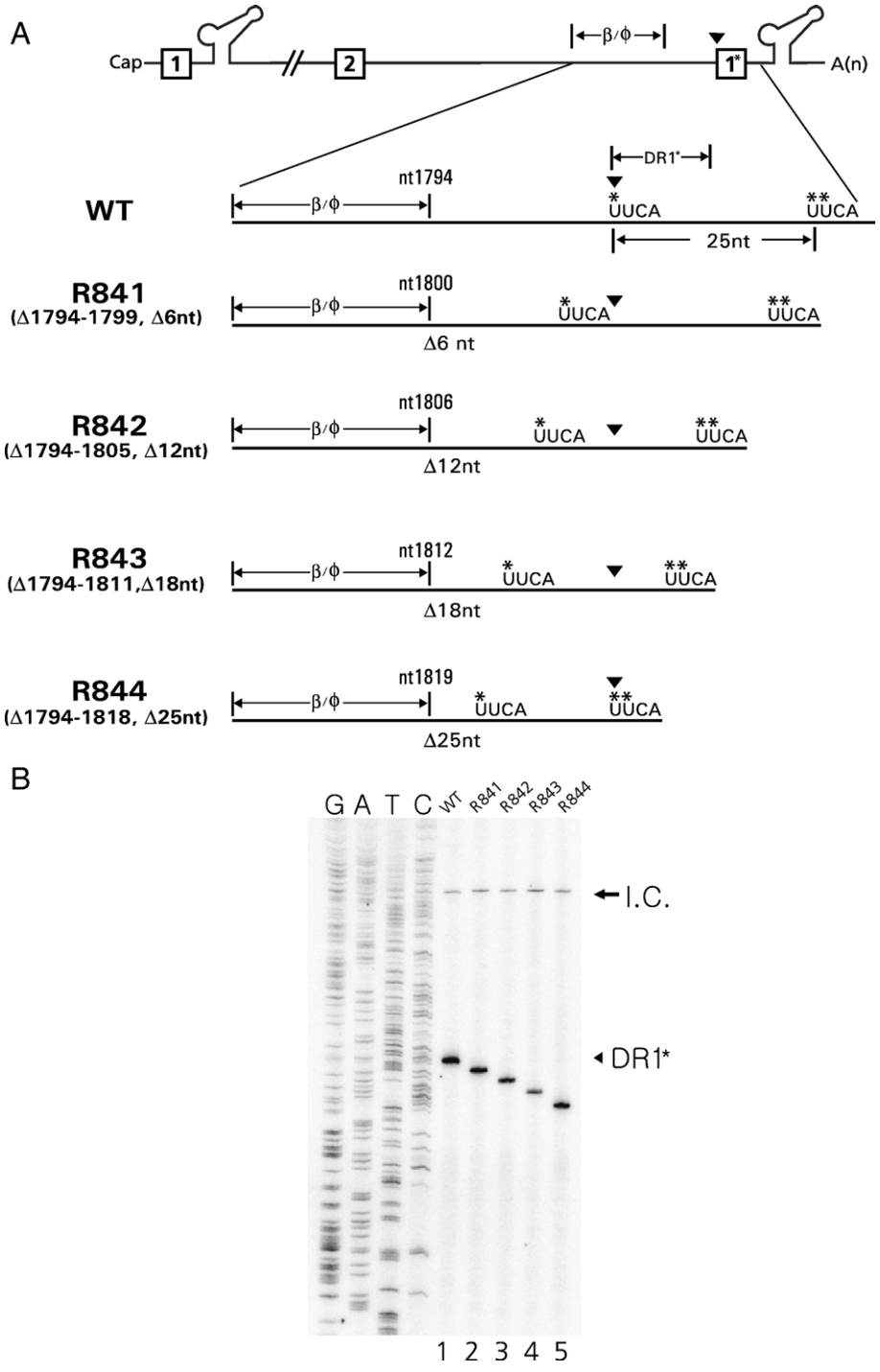

Fig. 6. A region spanning from the β/ϕ sequence to the DR1* sequence is dispensable for acceptor site selection during minus-strand synthesis. (A) Diagram showing four deletion mutants. The pgRNA, expanded below, shows the relative position of the UUCA sequences present downstream of the wild-type acceptor site at DR1*. The nucleotide sequences deleted in each mutant are indicated within parenthesis, with the corresponding deletion size. Two UUCA sequences are shown: one at DR1* (denoted by single asterisk) and another at 25 nucleotides away from the former (denoted by double asterisks). Closed triangles mark identical positions for the 5′ end; for example, in the R844 mutant, the next downstream UUCA sequence is relocated at the wild-type acceptor position with respect to the 5′ end. Symbols are as shown in Fig. 1. (B) Primer extension analysis was performed as shown in Fig. 3D to determine the 5′ termini of minus-strand DNAs.

detrimental to the viral genome replication than those in the β/ϕ sequences. However, it is unclear yet as to what is responsible for the discrepancy regarding the extent of the defects seen between these two groups of the single site mutants. Nevertheless, the substantive reduction of the minus-strand DNA synthesis seen in the single site mutants of the β/ϕ region further strengthened the interpretation made above. Overall, we concluded that the long-range base pairing between the 5′ ε and β/ϕ sequences is critical for the synthesis of minus-strand DNA.

A 7-nt sequence critical for the acceptor site selection

Having established the critical role of this 5′–3′ association, we next wanted to define the sequences that were critical for acceptor site selection. In other words, it is of considerable interest to determine how the wild-type UUC site of DR1* is selected among numerous UUC motifs present in pgRNA. In DHBV, a marked preference for the wild-type acceptor site was observed over numerous nearby UUC motifs (even over a site only 3 nt away) (Loeb and Tian, 1995). These data are consistent with the

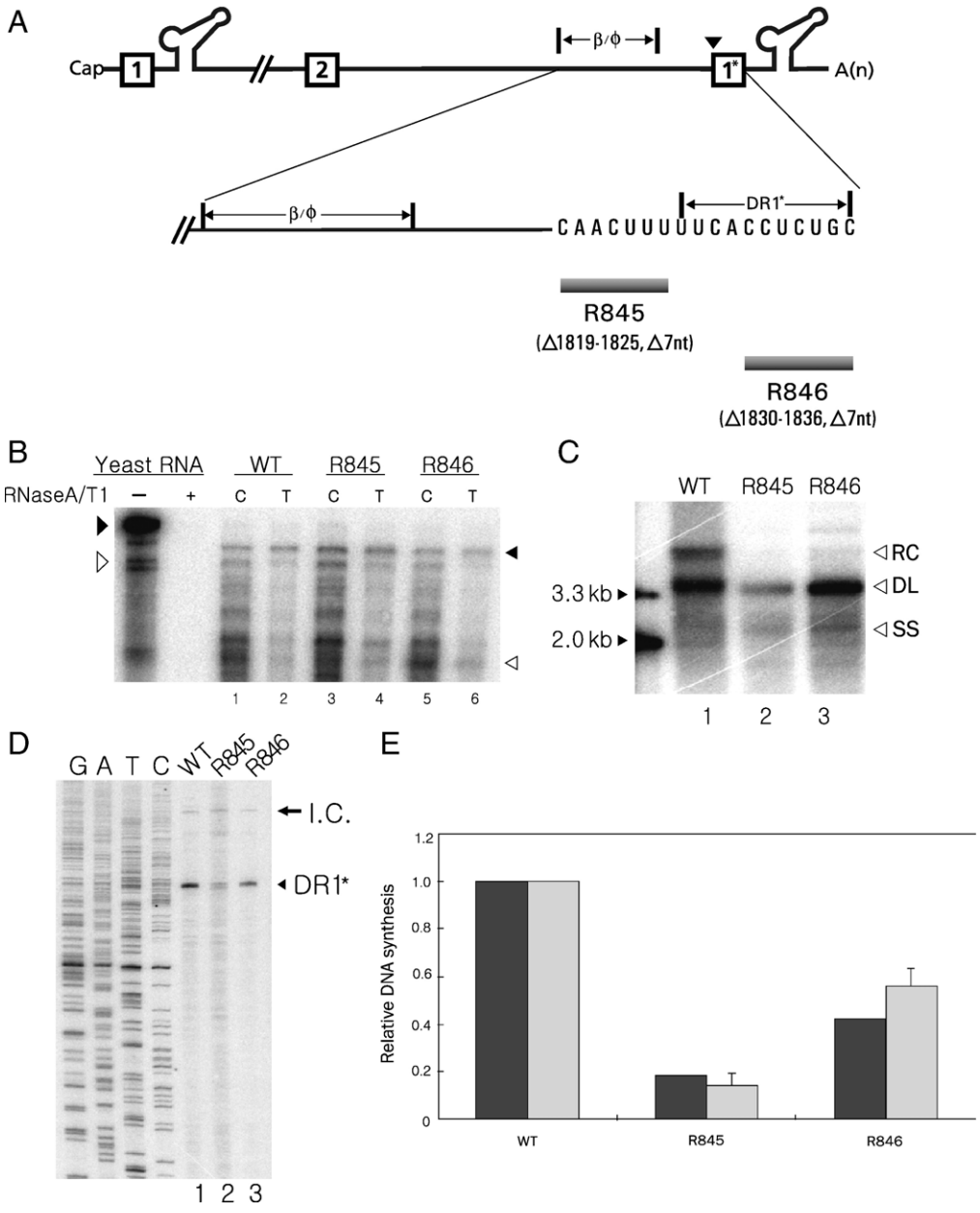

Fig. 7. Sequences flanking the wild-type acceptor site at DR1* are critical for acceptor site determination. (A) Two mutants lacking a 7-nucleotide sequence (shaded boxes), immediately adjacent to DR1*, are shown. Symbols are as shown in Fig. 1. (B) RPA analysis was performed as described in the Fig. 3B legend. (C) Southern blot analysis was performed as described in the Fig. 4C legend. (D) Primer extension analysis was performed as shown in Fig. 3D. (E) Quantitative analysis. The amounts of viral DNAs, as determined by Southern blot analysis (dark) or primer extension analysis (gray), were normalized to the amount of encapsulated RNA. Error bars represent standard deviations from four or more independent transfections.

interpretation that the P-pgRNA complex exerts a sort of measuring function (e.g., distance) in selecting the acceptor site.

To substantiate this idea, we asked whether the sequence that spans the β/ϕ sequence and the wild-type acceptor at DR1*, if any, contributes to acceptor site selection. To this end, we made four small deletion mutants that lacked 6 to 25 nucleotides (Fig. 6A). Particularly for the R844 mutant, a 25-nucleotide deletion was made, such that the next downstream UUC motif was newly positioned at the location of the wild-type UUC site with respect to the β/ϕ sequence. If the physical distance from the β/ϕ sequence to the UUC motif is a critical determinant for acceptor selection, we expected the downstream UUC motif at nucleotide 1851 to be utilized.

Primer extension analysis revealed that the extension products that were detected for each mutant were predictably shorter than those of the wild type, implying that the minus-strand DNA transferred to DR1* rather than the downstream UUC sequence (Fig. 6B). In other words, the wild-type UUC motif was used as an acceptor for all four mutants. It appeared that the region that spanned from the β/ϕ sequence to the DR1* sequence was largely dispensable for acceptor site selection. We interpreted these data as indicating that the sequences immediately adjacent to the UUC motif instead are more important.

To evaluate the contribution of sequences surrounding the UUCA sequence at DR1*, we generated two mutants that lack 7-nucleotide sequences that flank either upstream or downstream of the UUCA sequence at DR1*: (i) a 7-nucleotide sequence that spans from the β/ϕ sequence to the DR1* sequence in R844 was deleted in the R845 mutant (Fig. 7A), and (ii) a 7-nucleotide sequence that represents the DR1* sequence except for the wild-type acceptor (UUCA) was deleted in the R846 mutant (Fig. 7A). Transfection was performed as described above. RPA confirmed that encapsidation proceeded normally in these mutants (Fig. 7B). Southern blot analysis indicated that the R845 mutant yielded a markedly reduced amount of viral DNA, whereas the reduction was less pronounced in the R846 mutant transfected cells (Fig. 7C). In addition, primer extension analysis detected coordinate reductions in the amount of minus-strand DNA initiated at DR1* in the two mutants (Fig. 7D). Quantification that followed normalization of the encapsidated RNA further confirmed the above results (Fig. 7E). Based on these findings, we concluded that the 7-nucleotide sequence that was located immediately upstream of the UUCA at DR1* was critical in selecting the acceptor site during minus-strand transfer; this 7-nucleotide sequence was termed here as the acceptor determining sequence (*ads*).

Discussion

Strand transfer (or template switching) is a hallmark of the reverse transcription reaction that is employed by retrovirus-like elements including hepadnaviruses (Telesnitsky and Goff, 1997). Although the donor and the acceptor sites have been defined both for minus- and plus-strand DNA transfer, the mechanism of template switching has been enigmatic for some time. In the case of plus-strand DNA transfer, however, mechanistic insight has been provided by Loeb and his colleagues in that a long-range base pairing between appropriate sequence elements is critical, which could bring the donor into close proximity with the acceptor to facilitate transfer (Lewellyn and Loeb, 2007; Liu et al., 2003). In contrast, a parallel finding has not been made for minus-strand transfer.

Here, we asked how the β/ϕ sequence (Shin et al., 2004; Tang and McLachlan, 2002), a recently identified, novel *cis*-acting element, acts to facilitate minus-strand DNA synthesis. We provided experimental evidence for the hypothesized closed-loop RNA structure that involves a long-range base pairing between the 5′ ε and β/ϕ sequences (Fig. 4). Similar conclusions have been recently obtained by others (Abraham and Loeb, 2006; Oropeza and McLachlan, 2007). More recently, another *cis*-acting element that is engaged in the long-range base pairing was reported (Abraham and Loeb, 2007); the third *cis*-acting element, called ω element, is located immediately 3′ to the acceptor site. Possibly, the P-pgRNA complex that undergoes conformational alteration upon priming might direct a juxtaposition of the donor to the acceptor that is present at opposite ends of the RNA template. Perhaps, the precise juxtaposition of the donor to the acceptor is a critical constraint that is imposed on the RNA template during minus-strand transfer. We further speculate that a precise juxtaposition could be achieved via a triple-strand helices (triplex) formation (Fig. 8).

Presently, how exactly the 5′ ε sequence that folds into a stable stem-loop structure could interact with the β/ϕ sequence via base pairing remains uncertain. Perhaps upon priming, the 5′ ε stem-loop structure undergoes structural alterations (melting) such that the β/ϕ sequence could invade and anneal to an appropriate part of the 5′ ε sequence. In fact, evidence is available in DHBV to suggest that both the stem-loop structure and P protein undergo marked structural rearrangements that accompany the melting of the upper stem (Beck and Nassal, 1998; Tavis and Ganem, 1996). In particular, the melting of the 5′ ε upper stem precedes the formation of a replication-competent P-ε complex (Beck and Nassal, 1998). In keeping with this idea, we observed that the upper stem in the hypothesized structure shown in Fig. 2A is more critical than the lower stem for minus-strand DNA synthesis (data not shown). In fact, a lesser importance of the lower stem was anticipated by Tang and McLachlan (2002), as the lower stems found in mammalian hepadnaviruses are not conserved in DHBV.

How then is the acceptor site selected from numerous UUC motifs present on the pgRNA? A marked preference for the wild-type acceptor site implied a limited flexibility in selecting the site of transfer (Loeb and Tian, 1995). In this regard, our results argue that the constraints in selecting the acceptor are primarily imparted by sequences surrounding the acceptor site (Fig. 6). Subsequent deletion analysis defined a 7-nucleotide element (*ads*) that directs acceptor site selection (Fig. 7). In fact, only subset of the 7-nt could be critical for the acceptor site selection. In parallel, a hexanucleotide (AA*UUAC*; the acceptor site italicized) was previously identified in DHBV as the primary *cis* element that direct the acceptor site selection (Tavis and Ganem, 1995). Importance of a short stretch sequence (2 or more nt) immediately upstream to the acceptor site appears to be a conserved features between avian and mammalian hepadnaviruses. Possibly, the viral P protein specifically recognizes the *ads* sequence and

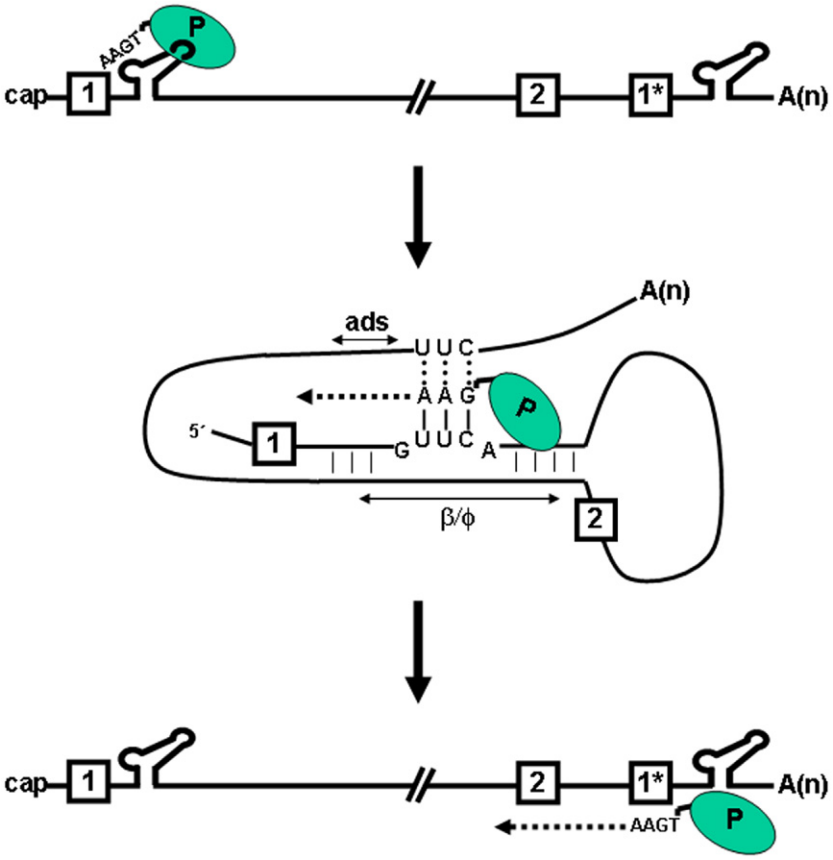

Fig. 8. Schematic model illustrating the minus-strand transfer of hepadnaviruses. We hypothesized that the base pairing between the 5′ ε and β/ϕ sequences mediates the precise juxtaposition of the donor to the acceptor via triple helix formation. A hypothesized triplex consists of the P-linked trinucleotides (5′-GAA-3′) that link the donor (5′-UUC-3′) and the acceptor (5′-UUC-3′). Hoogsteen base pairing is denoted by dotted lines, whereas Watson–Crick base pairing is denoted by solid lines. *ads*: acceptor determining sequence. Symbols are as shown in Fig. 1.

facilitate the strand transfer (Fig. 8). On the other hand, the *ads* sequence happens to overlap the *r* (repeat) sequence element, which is critical for template switching that occurs during plus-strand DNA synthesis (Habig and Loeb, 2003; Loeb et al., 1997). It should be noted, however, that the *ads* sequence acts at the RNA level, whereas the *r* sequence acts at the DNA level. Thus, it is unlikely that these two elements are mechanistically related.

What is the exact mechanism whereby strand transfer or template switching occurs at the growing end? From the viral perspective, it is crucial to avoid copying an extra base at the 5′ ε bulge region, as the P-linked oligomer would otherwise fail to translocate to DR1* due to a mismatched base at the 3′ end (Fig. 8). Conformational alteration was suggested by earlier observation that noted altered sensitivity of the P protein to PFA (phosphonoformate) in vitro reaction: from PFA resistance to PFA sensitive (Wang and Seeger, 1992). We consider it possible that, following oligomer synthesis, the P protein undergoes a drastic conformational alteration that accompanies template switching from the donor to the acceptor. One could even speculate that a triple-stranded intermediate is formed that involves the newly synthesized oligomer (Fig. 8). A triple-stranded helix has been, in fact, demonstrated for T7 DNA polymerase (Rocher et al., 2001). Triplexes typically are composed of polypurine- or polypyrimidine-rich sequences, where not only Watson–Crick base pairs but also Hoogsteen base pairs are involved (Frank-Kamenetskii and Mirkin, 1995). Possibly, the P-linked oligomer could interact with the donor via Watson–Crick base pairs, but simultaneously could interact with the acceptor via Hoogsteen base pairs or vice versa. According to this scenario, strand transfer merely represents a process of changing the Watson–Crick base pairing partner of the P-linked oligomer from the donor to the acceptor (Fig. 8). Certainly, experimental evaluation of this triplex hypothesis requires further investigation.

In fact, a 5′–3′, long-range RNA-RNA interaction for reverse transcription is not unprecedented. A parallel, 5′–3′, long-range base pairing interaction was shown to be critical for the initiation of minus-strand DNA synthesis in Ty1 RNA (Cristofari et al., 2002), a retrotransposon in budding yeasts. Moreover, a recent study reported that a 5′–3′ association via a lariat-like structure, involving a covalent 2′–5′ linkage, was found during reverse transcription of Ty1 RNA (Cheng and Menees, 2004). Although the underlying molecular mechanisms are not mechanistically related, circularization of an RNA template appeared to be a conserved strategy to facilitate template switching commonly adopted by hepadnaviruses and Ty elements during evolution (Fig. 8). Whether the circularization strategy could be extended to retroviruses is a matter of speculation.

Evidently, identification of the *cis*-acting element that is critical for hepadnaviral minus-strand transfer has provided an important clue toward a more complete molecular description of strand transfer events. We now present an insight into how *cis*-acting elements contribute to strand transfer. A detailed understanding of hepadnaviral minus-strand transfer will provide not only new insight into our understanding of RNA-directed DNA synthesis, but also possibly uncover new targets for therapeutic antiviral intervention.

Materials and methods

Cell culture and transfection

The human hepatoma cell lines, Huh7 and HepG2, were cultured as previously described (Lee et al., 2004b). Plasmid DNAs were transfected into cells by calcium phosphate transfection (Jeong et al., 2000).

Plasmid construction

All HBV constructs were derived from a wild-type HBV expression clone, pCMV-HBV/30 plasmid as previously described (Jeong et al., 2000). The nucleotide sequence of the HBV genome was numbered starting from the unique *Eco*RI site of the HBV ayw subtype (Galibert et al., 1979). In this numbering system, the 5′ end of the pregenomic RNA is at nt 1820 (Nassal et al., 1990). All substitution and deletion mutants were generated by overlap extension PCR protocol as previously described (Lee et al., 2004a). The details of the molecular cloning of any plasmid construct will be provided upon request. All mutants were sequenced to confirm the base change. The helper plasmid, R063, is designed to yield the pgRNA lacking the encapsidation signal (5′ ε) as previously described (Jeong et al., 2000).

Isolation of encapsidated RNA

Cells were transfected with each mutant along with a helper plasmid, R063. To account for variation between plates, we extracted both capsid RNA and total cytoplasmic RNA from a single plate. A day following transfection, cells were treated with lamivudine (20 μM) for 48 h before harvest. Cells were lysed with lysis buffer (10 mM Tris [pH 8.0], 1 mM EDTA. 0.5% Nonidet P-40). One fifth of the lysate was used to isolate the total cytoplasmic RNA, while the rest was used to isolate the capsid RNA. RNA extraction was performed essentially as previously described (Jeong et al., 2000).

RNase protection assay

RNA extraction and RNase protection assay (RPA) was performed essentially as previously described (Jeong et al., 2000). Briefly, samples of total RNA (30 μg) or core-associated RNA were hybridized with two [α-^{32} P]UTP(3000 Ci/mmol; Amersham)-labeled probes for 16 h at 42 °C. RNase digestions were carried out with a mixture of RNase A and RNase T1 (Ambion) at 37 °C for 30 min. The digested products were separated on a 6% acrylamide-8 M urea gel. The gels were dried and autoradiographed on Hyperfilm-MP (Amersham) at −70 °C. Phosphorimages were quantified using a bio-imaging analyzer (BAS-2500; Fujifilm). The RNA probe used to detect HBV-specific pgRNAs was generated by the in vitro transcription of plasmid R654, which encodes the core coding sequence from nt 1909 to 2140. The *lacZ* RNA probe was used for these RNase protection analysis as previously described (Shin et al., 2004).

Isolation of viral DNAs

Viral DNAs from cytoplasmic capsids were isolated from Huh7 cells 3 days or from HepG2 cells 4 days, respectively, after transfection as described (Nassal, 1992). Half of the extracted DNA was used for Southern blot analysis, and the other half was used for primer extension analysis.

Southern blot analysis

Southern blot analysis was performed as previously described (Shin et al., 2004). Briefly, the extracted viral DNAs were electrophoresed through a 1.3% agarose gel in a 0.5× Tris-acetate-EDTA buffer. The membrane was prehybridized and hybridized with a ^{32}P-labeled full-length HBV DNA probe in a hybridization solution for 16 h at 65 °C. The membrane was autoradiographed with film (Hyperfilm-MP; Amersham) at −70 °C. Phosphorimages were quantified using a bio-imaging analyzer (BAS-2500; Fujifilm).

Primer extension analysis

Primer extension analysis was performed as previously described (Shin et al., 2004). Briefly, primer extension with the M2 primer [nt 1548–1570] was used to determine the 5′ end of minus-strand DNA from all substitution mutants and to measure the level of minus-strand DNA initiated at DR1*. Thermocycling parameters used for extension with M2 primer were 20 cycles of 95 °C for 40 s, 54.5 °C for 40 s and 72 °C for 40 s. Samples were denatured at 95 °C for 5 min prior to electrophoresis through a 6% polyacrylamide-8 M urea sequencing gel. Gels were dried and autoradiographed with Hyperfilm-MP (Amersham) at −70 °C.

Acknowledgments

We thank Drs. Byung-Yoon Ahn (Korea University) and Jehan Lee (Yonsei University) for their critical reading of this manuscript. This work was supported by the Korean Research Foundation Grant (MOEHRD) (KRF-2004-041-C00286).

References

Abraham, T.M., Loeb, D.D., 2006. Base pairing between the 5′ half of epsilon and a *cis*-acting sequence, phi, makes a contribution to the synthesis of minus-strand DNA for human hepatitis B virus. J. Virol. 80 (9), 4380–4387.

Abraham, T.M., Loeb, D.D., 2007. Topology of HBV pregenomic RNA promotes its replication. J. Virol. 81 (21), 11577–11584.

Beck, J., Nassal, M., 1998. Formation of a functional hepatitis B virus replication initiation complex involves a major structural alteration in the RNA template. Mol. Cell. Biol. 18 (11), 6265–6272.

Cheng, Z., Menees, T.M., 2004. RNA branching and debranching in the yeast retrovirus-like element Ty1. Science 303 (5655), 240–243.

Cristofari, G., Bampi, C., Wilhelm, M., Wilhelm, F.X., Darlix, J.L., 2002. A 5′–3′ long-range interaction in Ty1 RNA controls its reverse transcription and retrotransposition. EMBO J. 21 (16), 4368–4379.

Dang, Q., Hu, W.S., 2001. Effects of homology length in the repeat region on minus-strand DNA transfer and retroviral replication. J. Virol. 75 (2), 809–820.

Fallows, D.A., Goff, S.P., 1995. Mutations in the epsilon sequences of human hepatitis B virus affect both RNA encapsidation and reverse transcription. J. Virol. 69 (5), 3067–3073.

Frank-Kamenetskii, M.D., Mirkin, S.M., 1995. Triplex DNA structures. Ann. Rev. Biochem. 64, 65–95.

Galibert, F., Mandart, E., Fitoussi, F., Tiollais, P., Charnay, P., 1979. Nucleotide sequence of the hepatitis B virus genome (subtype ayw) cloned in E. coli. Nature 281 (5733), 646–650.

Ganem, D., Schneider, R., 2001. In: Knipe, P.M.H.D.M. (Ed.), 4th ed. Hepadnaviridae: The Viruses and Their Replication, vol. 2. Lippincott-Raven Publishers, Philadelphia, pp. 2923–2970 (2 vols.).

Habig, J.W., Loeb, D.D., 2003. Template switches during plus-strand DNA synthesis of duck hepatitis B virus are influenced by the base composition of the minus-strand terminal redundancy. J. Virol. 77 (23), 12412–12420.

Hirsch, R.C., Loeb, D.D., Pollack, J.R., Ganem, D., 1991. *cis*-Acting sequences required for encapsidation of duck hepatitis B virus pregenomic RNA. J. Virol. 65 (6), 3309–3316.

Jeong, J.K., Yoon, G.S., Ryu, W.S., 2000. Evidence that the 5′-end cap structure is essential for encapsidation of hepatitis B virus pregenomic RNA. J. Virol. 74 (12), 5502–5508.

Junker-Niepmann, M., Bartenschlager, R., Schaller, H., 1990. A short *cis*-acting sequence is required for hepatitis B virus pregenome encapsidation and sufficient for packaging of foreign RNA. EMBO J. 9 (10), 3389–3396.

Lee, J., Lee, H.-J., Shin, M.-K., Ryu, W.-S., 2004a. Versatile PCR-mediated insertion or deletion mutagenesis. BioTechniques 36 (3), 398–400.

Lee, J., Shin, M.-K., Lee, H.-J., Yoon, G., Ryu, W.-S., 2004b. Three novel *cis*-acting elements required for efficient plus-strand DNA synthesis of the hepatitis B virus genome. J. Virol. 78 (14), 7455–7464.

Lewellyn, E.B., Loeb, D.D., 2007. Base pairing between *cis*-acting sequences contributes to template switching during plus-strand DNA synthesis in human hepatitis B virus. J. Virol. 81 (12), 6207–6215.

Liu, N., Tian, R., Loeb, D.D., 2003. Base pairing among three *cis*-acting sequences contributes to template switching during hepadnavirus reverse transcription. PNAS 100 (4), 1984–1989.

Loeb, D.D., Tian, R., 1995. Transfer of the minus strand of DNA during hepadnavirus replication is not invariable but prefers a specific location. J. Virol. 69 (11), 6886–6891.

Loeb, D.D., Gulya, K.J., Tian, R., 1997. Sequence identity of the terminal redundancies on the minus-strand DNA template is necessary but not sufficient for the template switch during hepadnavirus plus-strand DNA synthesis. J. Virol. 71 (1), 152–160.

Nassal, M., 1992. The arginine-rich domain of the hepatitis B virus core protein is required for pregenome encapsidation and productive viral positive-strand DNA synthesis but not for virus assembly. J. Virol. 66 (7), 4107–4116.

Nassal, M., Rieger, A., 1996. A bulged region of the hepatitis B virus RNA encapsidation signal contains the replication origin for discontinuous first-strand DNA synthesis. J. Virol. 70 (5), 2764–2773.

Nassal, M., Junker-Niepmann, M., Schaller, H., 1990. Translational inactivation of RNA function: discrimination against a subset of genomic transcripts during HBV nucleocapsid assembly. Cell 63 (6), 1357–1363.

Ono, S.K., Kato, N., Shiratori, Y., Kato, J., Goto, T., Schinazi, R.F., Carrilho, F.J., Omata, M., 2001. The polymerase L528M mutation cooperates with nucleotide binding-site mutations, increasing hepatitis B virus replication and drug resistance. J. Clin. Invest. 107 (4), 449–455.

Oropeza, C.E., McLachlan, A., 2007. Complementarity between epsilon and phi sequences in pregenomic RNA influences hepatitis B virus replication efficiency. Virology 359 (2), 371–381.

Pollack, J.R., Ganem, D., 1993. An RNA stem-loop structure directs hepatitis B virus genomic RNA encapsidation. J. Virol. 67 (6), 3254–3263.

Pollack, J.R., Ganem, D., 1994. Site-specific RNA binding by a hepatitis B virus reverse transcriptase initiates two distinct reactions: RNA packaging and DNA synthesis. J. Virol. 68 (9), 5579–5587.

Rieger, A., Nassal, M., 1996. Specific hepatitis B virus minus-strand DNA synthesis requires only the 5′ encapsidation signal and the 3′-proximal direct repeat DR1. J. Virol. 70 (1), 585–589.

Rocher, C., Dalibart, R., Letellier, T., Precigoux, G., Lestienne, P., 2001. Initiation of DNA replication by DNA polymerases from primers forming a triple helix. Nucleic Acids Res. 29 (16), 3320–3326.

Schaaf, S.G., Beck, J., Nassal, M., 1999. A small 2′-OH- and base-dependent recognition element downstream of the initiation site in the RNA encapsidation signal is essential for hepatitis B virus replication initiation. J. Biol. Chem. 274 (53), 37787–37794.

Shin, M.-K., Lee, J., Ryu, W.-S., 2004. A novel *cis*-acting element facilitates minus-strand DNA synthesis during reverse transcription of the hepatitis B viruses genome. J. Virol. 78, 6252–6262.

Tang, H., McLachlan, A., 2002. A pregenomic RNA sequence adjacent to DR1 and complementary to epsilon influences hepatitis B virus replication efficiency. Virology 303, 199–210.

Tavis, J., Ganem, D., 1995. RNA sequences controlling the initiation and transfer of duck hepatitis B virus minus-strand DNA. J. Virol. 69 (7), 4283–4291.

Tavis, J.E., Ganem, D., 1996. Evidence for activation of the hepatitis B virus polymerase by binding of its RNA template. J. Virol. 70 (9), 5741–5750.

Tavis, J.E., Perri, S., Ganem, D., 1994. Hepadnavirus reverse transcription initiates within the stem-loop of the RNA packaging signal and employs a novel strand transfer. J. Virol. 68 (6), 3536–3543.

Telesnitsky, A., Goff, S.P., 1997. Reverse transcriptase and the generation of retroviral DNA. In: Coffin, J.M., Hughes, S.H., Varmus, H.E. (Eds.), Retroviruses. Cold Spring Harbor Press, Cold Spring Harbor, pp. 121–160.

Wang, G.H., Seeger, C., 1992. The reverse transcriptase of hepatitis B virus acts as a protein primer for viral DNA synthesis. Cell 71 (4), 663–670.

Wang, G.H., Seeger, C., 1993. Novel mechanism for reverse transcription in hepatitis B viruses. J. Virol. 67 (11), 6507–6512.